

# Future of the Arctic Sea Ice Cover: Implications of an Antarctic Analog

Douglas G. Martinson

Lamont-Doherty Earth Observatory, and Department of Earth and Environmental Sciences, Columbia University, Palisades, NY 10964

Michael Steele

Polar Science Center, Applied Physics Laboratory, University of Washington, Seattle, WA 98105

**Abstract.** Recent observations reveal a significant change in the upper ocean characteristics of the eastern Arctic in 1995. The change is manifested through the loss of a near-surface layer known as the cold halocline layer (CHL). Without the CHL, the Arctic water column looks and behaves like the Antarctic water column. The expected local impact is the appearance of significant winter ocean heat fluxes ( $15 - 20 \text{ W/m}^2$ ) and reduction of winter ice growth by 70–80% relative to years in which the CHL was present. Preliminary results suggest a partial recovery of the CHL in the late 1990's, tracking the weakening of the Arctic Oscillation.

## Introduction

Numerous studies show that characteristics of the water column in the Arctic appear to be changing [e.g., *McLaughlin 1996, Carmack 1997*]. Of particular interest are those of *Steele and Boyd [1998; hereafter SB98]* who show a change in the structure of the near-surface waters in the mid-1990s. These waters typically consist of a shallow halocline that coincides with a near-freezing thermostad (Figure 1a). This is the cold halocline layer [CHL; *Aagaard 1981*]. *SB98* showed that the eastern-central Arctic CHL was unusually weak in 1993 and absent in 1995 (Figure 1).

The Antarctic Ocean has no permanent CHL. In this regard, the Arctic CHL loss creates a situation wherein the two oceans may exhibit similar upper ocean behavior. In particular, we are concerned with the ability of the ocean to influence sea ice through the exchange of heat at the air-ice-ocean interface. We focus here on the ocean heat flux that occurs in winter after the seasonal pycnocline is eliminated by fall ice growth.

In the Antarctic's Weddell gyre, the average winter flux,  $\langle F_T \rangle = 25 - 40 \text{ W/m}^2$ , or annually,  $10 - 17 \text{ W/m}^2$  [e.g., *Gordon 1990, Martinson 1990*]. This is sufficient to melt, or prevent from forming,  $\sim 1.5\text{m}$  of ice each winter and is partly responsible for the Antarctic's thin seasonal sea ice cover. Conversely, where a CHL exists, the thick perennial Arctic sea ice partially reflects its minimal ocean-ice interaction, with  $\langle F_T \rangle \leq 0.7 \text{ W/m}^2$ , or annually,  $\leq 0.3 \text{ W/m}^2$  [*Morison and Smith, 1981*], although significant fluxes may occur during winter on the shelves [*Zhang et al., 1998a*].

The  $\langle F_T \rangle$  difference between the two polar regions is sometimes attributed to the fact that, unlike the Antarctic, the Arctic Ocean water column is strongly stabilized by a buoyant surface freshwater cap reflecting extensive riverine input and fresher North Pacific water inflow [*Aagaard and Carmack, 1989; Steele et al., 1996*]. Indeed, the Antarctic shows exceptionally weak vertical stability, with a density contrast between the winter surface waters and underlying deep waters (i.e., across the permanent pycnocline) of  $< 0.2\text{kg/m}^3$  in the Weddell region; the Arctic shows a density contrast often twice that or more. However, while the stability of the water column plays a role in the extent and nature of the ocean-ice interaction, more important is the relationship between salinity (S) and temperature (T) through the pycnocline.

Consider the Antarctic winter, where both S and T increase rapidly with depth when passing through the permanent pycnocline (c.f. Figure 1c). This leads to the following feedbacks. First, ice growth releases salt to the water, which increases surface layer density introducing a static instability that is relieved by convection to a new stable depth. The convection mixes pycnocline water into the mixed layer, where excess enthalpy relative to the freezing point is made available as sensible heat to the surface, either melting some of the ice that just grew or accomplishing the equivalent by preventing a comparable amount of new growth.

This buoyancy-driven negative feedback mechanism is effective in venting deep ocean heat and reducing winter ice growth. It complements the turbulent diffusive heat flux forced by shear (generated by surface stress, tides, eddies, and internal waves). In the Weddell gyre region, the combination of diffusive and entrainment heat fluxes are sufficient to supply nearly all of the winter air-sea heat flux, keeping net winter ice growth to negligible levels [*Martinson, 1990*] and limiting the ice cover to predominantly that formed during the fall.

When a CHL is present in the Arctic Ocean, entrainment into the upper levels of the pycnocline erodes the halocline and thermostad, but the latter is devoid of excess enthalpy and does not introduce additional heat into the mixed layer. Consequently, the negative feedback mechanism is inoperative. However, removal of the CHL exposes the ocean's surface layer directly to the warm thermocline, allowing significant Antarctic-like winter ocean heat fluxes with commensurate reduction in ice growth.

## Estimating Mean Ocean Heat Fluxes

The magnitude of the seasonally-averaged winter sensible ocean heat flux ( $\langle F_T \rangle$ ) is estimated using the net ther-

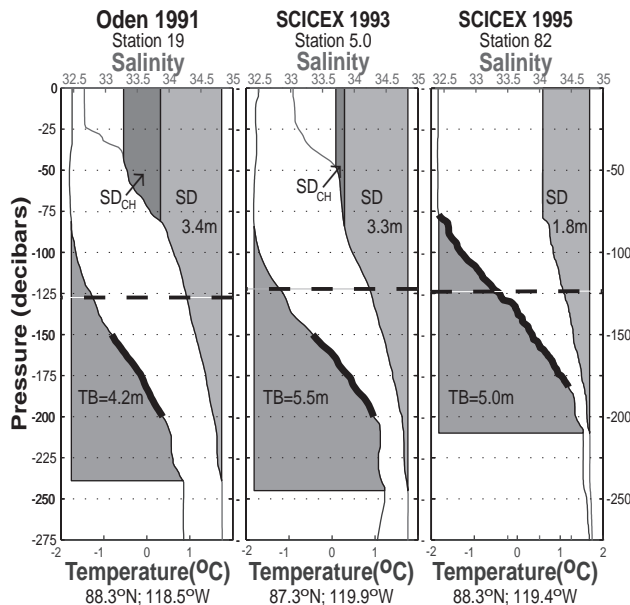


**Figure 1.** Eastern Arctic profiles (located in Figure 2) acquired in 1991, 1993 and 1995 near the North Pole. CHL is weak but present in 1993 and absent in 1995 profile. Shaded areas show important characteristics of upper water column: cold halocline layer (CHL), TB (thermal barrier) and SD (salt deficit). Dashed lines indicate depth of winter convection; bold portion of T profiles indicate portion of pycnocline, unaffected by presence of CHL

mal forcing in combination with parameters derived from vertically integrated upper ocean T and S profiles. The method, developed by *Martinson and Iannuzzi* [1998; hereafter *MI98*], for Antarctic polar waters, arises from previously derived scaling laws [*Martinson, 1990*] and assumes that ocean-ice interactions reflect, when averaged over appropriate space/time scales, a balance of vertical processes.  $\langle F_T \rangle$  estimates agree well with observed values [c.f., *MI98* to *McPhee et al., 1999*].

The net thermal forcing for winter ice growth,  $F_L$ , is generated by the upward flux of heat at the bottom of the atmosphere,  $F_a$ , less the upward flux of oceanic heat into the mixed, layer created by diffusion,  $F_D$ . Seasonally-averaged values (indicated by  $\langle \rangle$ ) of these fluxes are provided as inputs to the bulk parameterization, which then calculates the additional heat flux  $\langle F_E \rangle$  that can occur when surface convection forces entrainment of warm water from below the mixed layer. The total ocean sensible heat flux is  $\langle F_T \rangle = \langle F_D \rangle + \langle F_E \rangle$ .

The diffusive heat flux is parameterized as proportional to the thermal gradient through the thermocline:  $\langle F_D \rangle = \rho_p \langle k_z \rangle \nabla T$ . The seasonally-averaged winter turbulent diffusion coefficient,  $\langle k_z \rangle$ , across the pycnocline is large in the Antarctic (see *MI98*),  $\sim 0.6 \times 10^{-4} \text{ m}^2/\text{s}$ , reflecting small values during quiescent periods averaged with substantially increased values during frequent Antarctic storms. For the Arctic, *SB98* modeled the complex turbulent mixing processes. Their computed fluxes are comparable to  $\langle k_z \rangle \approx 0.2 \times 10^{-4} \text{ m}^2/\text{s}$ , which we use to estimate  $\langle F_D \rangle$  here.

The entrainment heat flux is estimated by examining the relationship between the surface freshwater content (relative to the salinity of the deep water), or “salt deficit” (SD), and

the enthalpy content (relative to the freezing point) of the thermocline, or “thermal barrier” (TB; see Figure 1). As ice grows, the rejected salt reduces SD, destabilizing the water column and venting heat stored within TB. For convenience, SD and TB are presented in terms of ice thickness: how much ice would have to grow to eliminate SD (assuming 5ppt ice salinity) and how much ice TB would melt if completely vented. *MI98* show that  $\langle F_E \rangle = \langle F_L \rangle TB/\Sigma$ , where  $\Sigma = SD + TB$  is the water column’s bulk stability.

The algorithm was modified from its original Antarctic formulation in the following ways. Where it exists, the CHL tends to cool the upper pycnocline, thus affecting our estimates of potential heat flux if the CHL were to vanish. We addressed this by substituting deeper mid-pycnocline slopes for the upper pycnocline in these conditions (Figure 1). We also reduced SD and TB to account for the relatively weak convection that occurs over the 5 months of winter in strongly stable Arctic conditions. A final correction might be made to account for the evolution of SD over the winter of 1995 as the mixed layer remained deep but salt was added via ice growth. This was not done; we estimate an average resulting  $\langle F_E \rangle$  overestimate of 5% for 1995 estimates.

## Results

We apply our bulk analysis to the Arctic stations presented in *SB98*, which sample 1991, 1993 and 1995. Figure 1 presents T and S profiles from three stations acquired near the North Pole in three different years. The 1995 profile has no CHL and is analogous to Antarctic profiles. For this 1995 profile,  $TB = 5 \text{ m}$ ,  $SD = 1.8 \text{ m}$ ,  $\Sigma = 6.8 \text{ m}$  and  $\langle F_D \rangle = 2.2 \text{ W/m}^2$ . *Overland et al.* [1997] find  $\langle F_a \rangle \approx 25 \text{ W/m}^2$  in which case the net thermal forcing is  $\langle F_L \rangle = \langle F_a \rangle - \langle F_D \rangle = 22.8 \text{ W/m}^2$ .

This initial ice growth drives an entrainment heat flux of  $\langle F_E \rangle = 22.8 * TB/\Sigma = 16.8 \text{ W/m}^2$ . Together,  $\langle F_E \rangle$  and  $\langle F_D \rangle$  yield a net ocean sensible heat flux  $\langle F_T \rangle = 19 \text{ W/m}^2$ , which reduces the latent heat flux associated with ice growth from a maximum potential of  $\langle F_a \rangle = 25 \text{ W/m}^2$  to  $\langle F_a \rangle - \langle F_T \rangle = 6 \text{ W/m}^2$ , a decrease of 76%! This fractional reduction is  $\Theta_r = \langle F_T \rangle / \langle F_a \rangle = (SD/\Sigma) \langle F_D \rangle / \langle F_a \rangle + TB/\Sigma$ , where the first term describes the decrease resulting from diffusion (in this example, only 1%) and the second term describes the decrease resulting from entrainment (in this example, 75%).

The total ocean heat flux thus reduces absolute winter ice growth by  $\Delta h = \rho_i L \Theta_r \Delta t \langle F_a \rangle = 1.1 \text{ m}$  for this example, where  $\rho_i$  and  $L$  are ice density ( $900 \text{ kg/m}^3$ ) and latent heat of fusion ( $2.54 \times 10^5 \text{ J/kg}$ ), and  $\Delta t = 5$  months. This reduction in winter ice growth occurs only when the CHL is absent; thus we refer below to  $\langle F_T \rangle$  as the “ocean heat flux potential”. (Note that “winter” is defined here as that time when the seasonal pycnocline is absent after removal by fall ice growth and the average upward air-ice heat flux is comparable to the upward ocean-ice heat flux. The latter occurs when  $\nabla T$  is nearly linear through the ice and snow so the conductive flux effectively transports heat from the ice bottom upwards. *Untersteiner* [1961] found this in multiyear ice from roughly mid-December to mid-May: 5 months.)

We next apply the analysis to the two earlier Arctic profiles in Figure 1 to estimate heat flux potentials given the loss of the CHL. The analysis proceeds by computing SD and TB

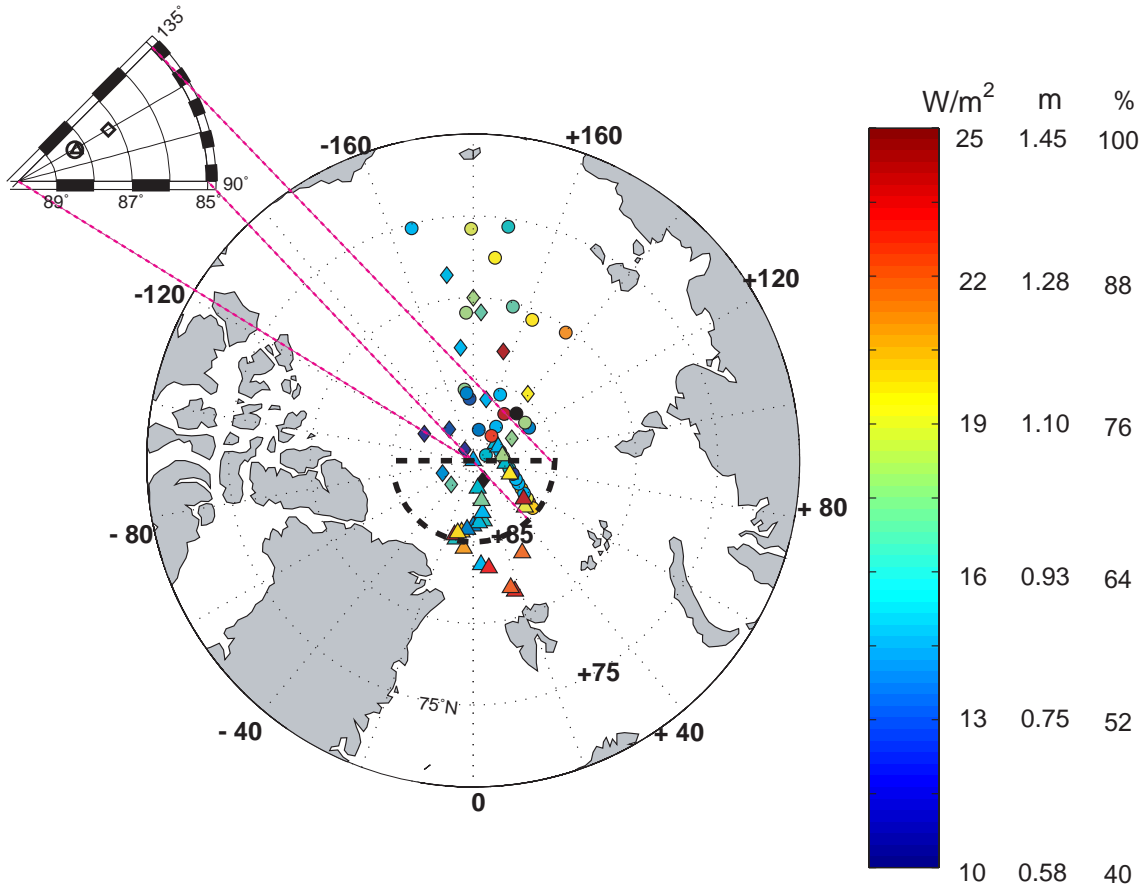


**Figure 2.** Station locations for three cruises used in this and original study of *Steele and Boyd* [1998] (triangles, squares and circles indicate: 1991, Oden; 1993, SCICEX, and 1995, SCICEX, cruises, respectively). Full Arctic domain includes all station locations. Dashed semi-circle indicates eastern Arctic domain, sampled by all cruises and where CHL was absent in 1995. Inset shows location of Figure 1 profiles. Color bar indicates: (left) Estimated seasonally-averaged winter ocean heat flux potential  $\langle F_T \rangle$ ; (middle) reduction in winter ice growth over 5-month winter period  $\Delta h$ ; and (right) percent reduction in winter ice growth  $\Theta_r$ , given loss of CHL relative to years with CHL present.

beneath the CHL, as if the CHL were not present. Results are indicated in Figure 1. The ocean heat flux potential  $\langle F_T \rangle$ , associated ice growth reduction  $\Delta h$ , and the per-

**Table 1.** Spatial Average Ocean-Ice Interaction.

		1991	1993	1995
Full Arctic	$\langle F_E \rangle$	$15.4 \pm 2.8$	$15.0 \pm 2.6$	$15.4 \pm 3.0$
	$\langle F_D \rangle$	$1.4 \pm 0.9$	$1.1 \pm 0.7$	$1.1 \pm 0.6$
	$\langle F_T \rangle$	$16.8 \pm 3.0$	$16.1 \pm 3.0$	$16.4 \pm 3.3$
	(%), $\Theta_r$	$67 \pm 12$	$64 \pm 12$	$66 \pm 13$
	(m), $\Sigma$	$8.7 \pm 2.9$	$12.0 \pm 5.2$	$10.2 \pm 4.5$
Eastern Arctic	$\langle F_E \rangle$	$14.2 \pm 3.6$	$18.0 \pm 0.3$	<b><math>17.6 \pm 1.0</math></b>
	$\langle F_D \rangle$	$1.3 \pm 0.5$	$1.4 \pm 0.5$	<b><math>1.8 \pm 0.3</math></b>
	$\langle F_T \rangle$	$15.5 \pm 2.7$	$19.5 \pm .03$	<b><math>19.4 \pm 1.0</math></b>
	(%), $\Theta_r$	$62 \pm 12$	$78 \pm 1$	<b><math>78 \pm 4</math></b>
	(m), $\Sigma$	$9.3 \pm 2.9$	$9.6 \pm 4.2$	<b><math>7.4 \pm 1.2</math></b>

Spatial average and range (one standard deviation about mean) of heat fluxes, ice growth reduction and other relevant values, for spatial domains of Figure 2.  $\langle F_E \rangle$  for 1995 may be  $\sim 5\%$  too high (because profiles were acquired in late winter).  $\langle F_E \rangle$ ,  $\langle F_D \rangle$ ,  $\langle F_T \rangle$  are entrainment, diffusive and total ocean heat flux, ( $W/m^2$ ).  $\Theta_r$  is ice growth reduction (%), and  $\Sigma$  is bulk stability (m of ice). Non-bold numbers provide potential values expected given loss of CHL.

cent reduction in winter ice growth potential  $\Theta_r$  throughout the Arctic are shown in Figure 2 and summarized in Table 1. Only for 1995 is this potential presumably realized since the CHL is absent. For these estimates  $\langle F_a \rangle = 25 W/m^2$  everywhere, introducing  $< 2\%$  error in  $\Theta_r$  since *Overland* [1997] show  $\langle F_a \rangle$  varies by  $\sim 5 W/m^2$  over the spatial domain of Figure 2. As seen,  $\langle F_T \rangle$  in 1991 and 1993 was comparable to that actually achieved (as estimated by our method) in 1995.

Table 1 reveals that areally-averaged potential heat fluxes are remarkably stable over the five year sampling window. Spatial variability is  $< 20\%$  over the full Arctic, though there appears to be a systematic decrease in heat flux potential heading toward the Chukchi Sea (Figure 2). Bulk parameter values show the largest change from 1991 to 1995 occurred in SD. While there were also changes in TB, the warmer deep water was offset by a shallower pycnocline base in 1995, minimizing the net change to TB. (Note that TB is defined as the heat content in the pycnocline, not the heat content of the entire Atlantic Water layer, a quantity which observations have shown did increase over the early 1990's.) This lends support to the mechanism proposed by *SB98* for elimination of the CHL whereby changes in the surface freshwater storage are forced by changes in the circulation of riverine-derived upper layers.

## Discussion and Conclusions

At present, it is not clear if the 1995 loss of the CHL in the eastern Arctic as shown by *SB98* is representative of a short-lived anomaly, long-term change, trend or cycle. Recent observations suggest that the CHL was still absent in 1996 [Schauer, personal communication], though preliminary findings suggest at least a partial recovery by 1999 [Muench, personal communication]. Its absence and potential recovery appears to mirror, to some extent, the strength and sign of the Arctic Oscillation [AO; Thompson and Wallace, 1998], which showed a strong positive peak in the mid-1990s before relaxing to lower values. Arctic modeling results [e.g., Zhang 1998b] suggest that the CHL loss reflects changes in ocean circulation and freshwater distribution in response to changed wind patterns. Global coupled simulations with increasing concentration of greenhouse gases [Fyfe et al., 1999] suggest a future with higher frequency of strongly positive AO, which leads us to speculate that the loss of the CHL may become more common in future years.

Regardless of the mechanism, it is clear that the CHL loss should introduce considerable ocean heat fluxes in winter, previously unknown in the Arctic. Unfortunately no measurements of actual winter fluxes are available for the CHL-free region. Changes in ice thickness may represent the only reasonable diagnostic of the activation of the ocean heat flux. In the absence of other changes, we estimate a corresponding reduction in winter ice growth from  $\sim 1.4$  m to  $0.3 - 0.4$  m, or  $70 - 80\%$ . However, this thinning is not applied to a single regionally-isolated slab of ice, but rather is spread over a considerable expanse of ice as it drifts over the affected area. Rothrock et al. [1999] and Johannessen et al. [1999] have recently shown that the Arctic ice pack is thinning. For 1993, 1996 and 1997, Rothrock et al. [1999] find more thinning each year with the highest loss in the area directly affected by the loss of the CHL. They show how some of this loss may derive from the increased advection of warm air associated with the increasing strength of the AO during the mid-1990s, and some from the increased ocean heat flux associated with the loss of the CHL.

**Acknowledgments.** We thank Dr. Robin Muench for allowing us to examine his preliminary CTD data from the 1999 SCICEX expedition. DGM's contribution was supported by National Science Foundation research grant OPP97-01383 and Ford Motor Company Environmental Research Grant 44024. MS's contribution was supported by NSF research grant OPP97-01592 and NASA grant NAG5-4375. Lamont-Doherty Earth Observatory number 6100.

## References

- Aagaard, K., L. Coachman and E. Carmack, On the halocline of the Arctic Ocean, *Deep Sea Res.*, 529, 1981.  
 Aagaard, K. and E.C. Carmack, The role of sea ice and other fresh water in the Arctic circulation, *J. Geophys. Res.*, 94, 14485-14498, 1989.

- Carmack, E. C., K. Aagaard, J. Swift, R. Macdonald, F. McLaughlin, E. Jones, R. Perkin, J. Smith, K. Ellis and L. Killius, Changes in temperature and tracer distributions within the Arctic Ocean: results from the 1994 Arctic Ocean section, *Deep Sea Res.*, 44, 1487, 1997.  
 Fyfe, J. C., G. J. Boer and G. M. Flato, The Arctic and Antarctic Oscillations and their projected changes under global warming, *Geophys. Res. Lett.*, 26, 1601-1604, 1999.  
 Gordon, A.L. and B.A. Huber, Southern Ocean Winter Mixed Layer, *J. Geophys. Res.*, 95, 11655-11672, 1990.  
 Johannessen O.M., E.V. Shalina, M.W. Miles, Satellite evidence for an Arctic sea ice cover in transformation, *Science*, 286, 1937-1939, 1999.  
 Martinson, D.G. and R. A. Iannuzzi, Antarctic Ocean-Ice Interaction: Implications From Ocean Bulk Property Distributions. In *Antarctic Research Series Volume on Antarctic Sea Ice Physical Properties and Processes*, AGU, edited by M. Jeffries, 74, 243-271, 1998.  
 Martinson, D.G., Evolution of the Southern Ocean winter mixed layer and sea ice: open ocean deepwater formation and ventilation, *J. Geophys. Res.*, 95, 11641-11654, 1990.  
 McLaughlin, F.A., E.C. Carmack, R.W. Macdonald and J.K.B. Bishop, Physical and geochemical properties across the Atlantic Pacific water mass front in the southern Canadian Basin, *J. Geophys. Res.*, 101 (c1), 1183, 1996.  
 McPhee, M., C. Kottmeier, and J. Morison, Ocean heat flux in the central Weddell Sea during winter, *J. Phys. Ocean.*, 29, 1166-1179, 1999.  
 Morison, J. and J. Smith, Seasonal variations in the upper Arctic Ocean as observed at T3, *Geophys. Res. Lett.*, 8, 753, 1981.  
 Overland, J.E. J.M. Adams, and N.A. Bond, Regional Variation of Winter Temperatures in the Arctic, *J. Clim.*, 10 821-837, 1997.  
 Rothrock, D.A., Y. Yu and G.A. Maykut, Thinning of the Arctic sea-ice cover, *Geophys. Res. Lett.*, 3469-3472.  
 Steele, M., and T. Boyd, Retreat of the cold halocline layer in the Arctic Ocean, *J. Geophys. Res.*, 10419-10435, 1998.  
 Steele, M., D. Thomas, D. Rothrock and S. Martin, A simple model study of the Arctic Ocean freshwater balance, 1979-1985, *J. Geophys. Res.*, 101 20833-20848, 1996.  
 Thompson D. and J.M. Wallace, The Arctic Oscillation signature in the wintertime geopotential height and temperature fields, *Geophys. Res. Lett.*, 25 (9), 1297-1300, 1998.  
 Untersteiner, N. On the mass and heat budget of Arctic sea ice, *Arch. Met. Geophys. Bioklimatol.*, 151, 1961.  
 Zhang, J., D. Rothrock and M. Steele, Warming of the Arctic Ocean by a strengthened Atlantic inflow: Model results, *Geophys. Res. Lett.*, 1745, 1998a.  
 Zhang, J., W.D. Hibler III, M. Steele and D.A. Rothrock, Arctic Ice-Ocean Modeling with and without Climate Restoring, *J. Phys. Ocean.*, 28 (2), 191-217, 1998b.

D.G. Martinson, Lamont-Doherty Earth Observatory, and Department of Earth and Environmental Sciences, Columbia University, Palisades, NY 10964

M. Steele, Polar Science Center, Applied Physics Laboratory, University of Washington, Seattle, WA 98105

(Received February 22, 2000; accepted July 11, 2000)